

## Experimental Investigations on Web Crippling Failure Modes of Aluminum Hollow and Composite Tubes

Xixiang Chen<sup>1</sup>, Yu Chen<sup>2,\*</sup>, Kang He<sup>2</sup> and Fernando Palacios Galarza<sup>3</sup>

**Abstract:** In order to study the web-crippling behavior of aluminum hollow section subjected to concentrated load, sixteen aluminum hollow tubes with different loading conditions, bearing length and web slenderness ratios were tested. This paper also discussed a method to improve the web crippling strength of the aluminum hollow sections by infilling the mortar as composite section, and four aluminum composite sections were tested. The literature has reported lots of web crippling tests, but there is few reports on web crippling behavior of aluminum composite sections. Interior-Ground (IG) and End-Ground (EG) loading conditions were adopted, with the specimens placed on the ground to simulate the load of floor joists. Specimens were also placed on a bearing plate with end (ETF) or interior (ITF) bearing load. The influence of supporting conditions, loading positions, bearing length and web slenderness ratios on web crippling ultimate bearing capacity and ductility of aluminum hollow sections was studied. The enhancements of infilling mortar were also evaluated. The results obtained from the experiments show that infilling the mortar in aluminum hollow tubes is an effective method for enhancing the ultimate capacity of the web, especially for specimens under Interior-Ground (IG) condition. Based on the results of parameter research, this paper proposes a series of design formulas for well predicting web crippling ultimate capacity of aluminum hollow and composite tubes under four different loading and boundary conditions.

**Keywords:** Web-crippling, aluminum hollow section, aluminum composite section, loading condition, bearing length, web slenderness ratio, ultimate capacity.

### 1 Introduction

Aluminum hollow sections have attracted extensive research attention. Due to the low elastic modulus of aluminum alloy, the web crippling is easy to occur when the aluminum hollow tube is subjected to concentrated load or load bearing reaction. Infilling the mortar in aluminum hollow tubes is an effective method for enhancing web crippling ultimate capacity of aluminum tubular sections.

The literature has reported a lot of web crippling tests. Zhou et al. [Zhou and Young

---

<sup>1</sup> College of Technology & Engineering, Yangtze University, Jingzhou, 434020, China.

<sup>2</sup> College of Civil Engineering, Fuzhou University, Fuzhou, 350116, China.

<sup>3</sup> School of Urban Construction, Yangtze University, Jingzhou, 434023, China.

\* Corresponding Author: Yu Chen. Email: kinkinging@163.com.

(2006)] presented an experimental study on web crippling performance of cold-formed stainless steel hollow sections. Bock et al. [Bock and Real (2014)] presented a new method for web crippling design of stainless steel hat sections. Web crippling tests of cold-formed steel lipped channel beams under four different loading conditions were investigated by Chen et al. [Chen, Chen and Wang (2015)]. Chen et al. [Chen and Wang (2015)] studied the web crippling properties of pultruded GFRP I-section. An experimental study on the web-crippling behavior in glass fiber reinforced polymer (GFRP) pultruded profiles with rectangular hollow section is presented by Chen et al. [Chen and Wang (2015)]. He et al. [He, Chen and Wan (2018)] proposed a number of design formulas, which can well predict web ultimate capacity of grouted galvanized steel tubes under four loading conditions. Parametric study of cold-formed steel sections with web openings under web crippling was carried out by Asraf et al. [Asraf, James and David et al. (2012)]. An experimental test and finite element analyses were used to study the influence of such holes on web crippling under interior-two-flange loading condition by Asraf et al. [Asraf, James, David et al. (2012)]. Natário et al. [Natário, Silvestre and Camotim (2014)] used quasi-static analyses with explicit integration to investigate the web crippling properties of cold-formed steel beams. Natário et al. [Natário, Silvestre and Camotim (2016)] developed a new method to predict the web crippling ultimate loads of cold-formed steel beams under End-Two-Flange loading condition. Web crippling behavior of high strength lipped channel beams subjected to one-flange loading were investigated by Lavan et al. [Lavan, Mahen and Poologanathan (2017)]. High strength steel tubular sections under four loading conditions were investigated by Li et al. [Li and Yang (2017)]. Zhou et al. [Zhou and Young (2008)] reported a lot of tests on aluminum square and rectangular hollow sections under web crippling. A experimental and parametric studies of aluminium square hollow sections with holes in the webs subjected to web crippling are presented by Zhou et al. [Zhou and Young (2010)]. Wu et al. [Wu and Bai (2014)] developed simple design formulas to evaluate the web crippling strength of pultruded GFRP sections. An experimental study on GFRP pultruded profiles with I-section subjected to web crippling has been proposed by Lourenço et al. [Lourenço, José and João et al. (2015)]. Macdonald et al. [Macdonald and Heiyantuduwa (2012)] developed a new rule for web crippling of cold-formed steel lipped channel beams.

On the other hand, Studies on improving web crippling strength have also been reported. Islam et al. [Islam and Young (2018)] performed a series of experimental tests and finite element analysis on carbon fibre-reinforced polymer stiffened aluminium tubular structural members under web crippling. Chen et al. [Chen, Chen and Wang (2016)] externally bonded CFRP sheets to galvanized steel tubular structural members, which strengthening of galvanized steel tubular. Islam et al. [Islam and Young (2014)] performed the laboratory and parametric studies of lean duplex stainless steel hollow sections strengthened with different fibre reinforced polymer subjected to web crippling. Islam et al. [Islam and Young (2013)] carried out a total of 58 web crippling tests of cold-formed stainless-steel tubular structural members strengthened with fibre-reinforced polymer subjected to ETF and ITF loading conditions. Lots of tests on CFRP strengthened aluminium hollow sections subjected to web crippling were conducted by Islam et al. [Islam and Young (2012)]. Islam et al. [Islam and Young (2011)] performed a lot of tests on aluminium tubular structural members strengthened with fiber reinforced

polymer subjected to ETF and ITF loading conditions. Wu et al. [Wu, Zhao and Duan (2011)] focused on proposing a series of design rules to predict the nominal crippling strength of CFRP strengthened sharp-corner aluminium tubular sections. Zhao et al. [Zhao and Al-Mahaid (2009)] presented the test results on CFRP- strengthened light steel beam under end-bearing loads.

However, there has been no report on web crippling behavior of grouted aluminum hollow tubes under four different loading and boundary conditions. In this paper, a comprehensive test, numerical study and design suggestions of grouted aluminum hollow tubes subjected to web crippling were carried out. Firstly, it is necessary to further investigate the ultimate bearing capacity, failure mode and ductility of grouted aluminum hollow tubes under web crippling. Secondly, the influence of variable depth-to-width ratio, different slenderness ratio, infilling the mortar in tube and loading conditions on web crippling behavior could be studied. Through the progressive failure process and load-displacement curves, the web crippling failure mechanisms of grouted aluminum tubes were revealed. Finally, a numerical investigation was performed using the general finite element analysis (FEA) program ABAQUS. The finite element model (FEM) included material and geometric nonlinearities; good agreements were found between the experimental results and the finite element analysis results. Through the verification of the finite element models, a series of parametric studies were carried out. The design equations of ultimate bearing capacity of grouted aluminium hollow tubes subjected to web crippling were also presented in this paper.

**2 Test procedures**

**2.1 Test specimens**

The web crippling tests were carried out on empty and grouted aluminum tubes with rectangular and square section. A total of 16 empty specimens and 4 grouted aluminum specimens were tested under transverse compressive loads as listed in Tab. 1.

**Table 1:** Relevant parameters of test specimens

Specimen number	Height <i>H</i> (mm)	Width <i>B</i> (mm)	Thickness of flange <i>t<sub>f</sub></i> (mm)	Thickness of web <i>t<sub>w</sub></i> (mm)	Slenderness ratio of web $\lambda=(H-2t_f-2r)/t_w$	Loading condition	Bearing length	Mortar strength <i>f<sub>cu</sub></i> (MPa)
100×100-EG-H-100	100.02	100.04	1.19	1.19	79.71	EG	100	0
100×100-ETF-H-100	100.02	100.00	1.21	1.20	78.98	ETF	100	0
100×100-IG-H-100	100.00	100.02	1.20	1.20	79.00	IG	100	0
100×100-ITF-H-100	100.02	100.00	1.18	1.21	78.43	ITF	100	0
110×65-EG-H-50	110.09	65.09	2.61	2.60	38.17	EG	50	0
110×65-EG-H-100	110.13	65.02	2.61	2.62	37.90	EG	100	0
110×65-EG-H-150	110.08	65.00	2.59	2.58	38.50	EG	150	0
110×65-ETF-H-50	110.06	65.00	2.62	2.61	38.00	ETF	50	0

110×65-ETF-H-100	109.96	65.02	2.61	2.60	38.12	ETF	100	0
110×65-ETF-H-150	110.12	65.08	2.59	2.58	38.51	ETF	150	0
110×65-IG-H-50	110.07	65.02	2.60	2.61	38.03	IG	50	0
110×65-IG-H-100	110.05	65.03	2.58	2.61	38.06	IG	100	0
110×65-IG-H-150	109.98	65.02	2.58	2.62	37.89	IG	150	0
110×65-ITF-H-50	110.02	64.98	2.60	2.61	38.02	ITF	50	0
110×65-ITF-H-100	110.02	65.00	2.60	2.62	37.87	ITF	100	0
110×65-ITF-H-150	110.09	65.01	2.61	2.59	38.32	ITF	150	0
110×65-EG-M-100	110.13	65.02	2.58	2.60	38.23	EG	100	15
110×65-ETF-M-100	110.10	65.00	2.59	2.61	38.06	ETF	100	15
110×65-IG-M-100	110.00	65.07	2.59	2.60	38.17	IG	100	15
110×65-ITF-M-100	110.02	65.02	2.60	2.61	38.02	ITF	100	15

The specimens were fabricated by aluminum tube with equal cross-section of SHS 100×100×1.2 mm and RHS 110×65×2.6 mm (height×width×thickness), as shown in Fig. 1. According to the requirements of ASCE Specification [American Society of Civil Engineers (2002)] and AS/NZS4673 [Australia Standards Association of Australia (2001)], the length of specimens should be at least 1.5 times larger than the web height. For the sake of convenience, the length of all specimens should be set to 500 mm.

The test specimens are labeled in accordance with major parameters. The first part is the cross-section size of 100×100 or 110×65. The second part indicates loading conditions, such as ETF refers to end-two-flange, ITF refers to interior-two-flange, EG refers to end bearing load with ground support and IG refers to interior bearing load with ground support. The third letter 'H' denotes aluminum hollow section. If there is 'M' in the label, it indicates mortar was filled in the aluminum tube. The last number denotes the length of the bearing plate.

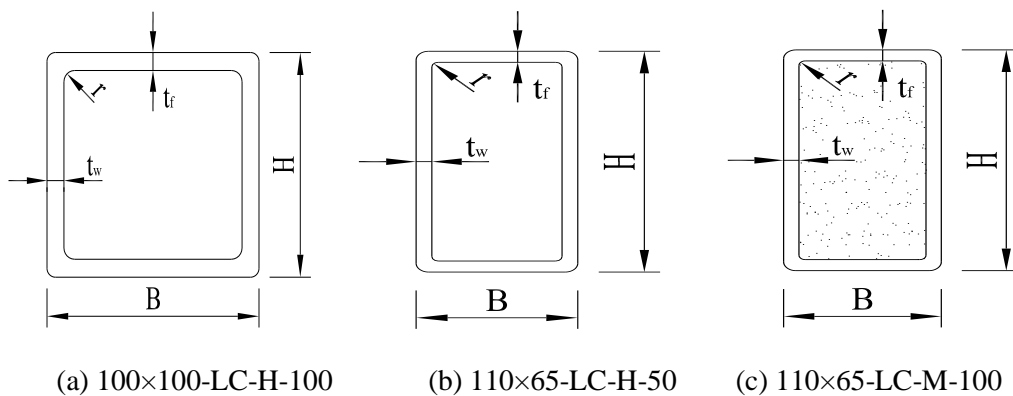


**Figure 1:** Section shapes and symbols

**2.2 Material properties**

The material characteristics of the aluminum specimens were determined by tensile test. The coupons were taken from the longitudinal center surface of the untested specimens and prepared in accordance with the recommendations of the Chinese Code of Metallic Materials (GB/T 228-2002) [Liang, Li, Tao et al. (2002)]. Tensile tests were carried out on a MTS displacement control instrument. The strain gauges were used to measure the longitudinal strains during the tests. The material characteristics obtained from the tensile coupon tests are shown in Tab. 2, including the elastic modulus ( $E$ ), the proof stress ( $f_{0.2}$ ), the ultimate tensile stress ( $f_u$ ), Poisson's ratio ( $\nu$ ) and the elongation after fracture ( $\epsilon_f$ ).

**Table 2:** Material characteristics of aluminum tubes

Specimens (mm×mm×mm)	$E$ (GPa)	$f_{0.2}$ (MPa)	$f_u$ (MPa)	$f_{0.2}/f_u$ (%)	$\nu$	$\epsilon_f$ (%)
100×100×1.2	71	157	182	0.86	0.32	8.38
110×65×2.6	76	186	204	0.91	0.30	10.18

The grouted specimens were formed by filling the mortar with nominal cube strength of 15 MPa into the entire tube. The material characteristics of mortar were determined by the compressive mortar cube tests. According to the suggestions of Standard for Test Method of Performance on Building Mortar (JGJ/T70-2009) [Li, Zhao, Wang et al. (2009)], the standard mortar cubes with a nominal length of 70 mm were prepared and tested. The material characteristics of the standard mortar cube are shown in Tab. 3, where the average value of the measured mortar cube strength ( $f_{mu}$ ) is 18.6 MPa.

**Table 3:** Material characteristics of mortar

Nominal mortar cube strength (MPa)	Specimens	Cube compressive Strength $f_{mu}$ (MPa)	Mean value $f_{mu}$ (MPa)
15	M-1	18.9	18.6
	M-2	18.5	
	M-3	18.4	

**2.3 Test scheme design**

All specimens were mounted on the same loading machine, as shown in Fig. 2. The self-balance reaction frame and supports were firmly attached to the sturdy floor by anchor bolts. The specimens were subjected to transverse compression loads by a 1000 kn hydraulic jack, which were monitored by a load measuring element located in the central position between the hydraulic jack and the self-balancing reaction frame. The concentrated load was applied by 30 mm thick rigid steel bearing plates, and the bearing length ( $b$ ) was 50 mm, 100 mm and 150 mm respectively in order to study the influence of different bearing lengths on web crippling strength. The width of the bearing plate was

300 mm enough to span the full flange widths of tubes. End-two-flange (ETF) and interior-two-flange (ITF) loading conditions were used, with specimens located on the bearing plate of the same length. Specimens were also seated on the ground with end (EG) or interior (IG) bearing load to simulate the load of floor joists, as shown in Fig. 3. Two displacement sensors (D1 and D2) were placed on the load-bearing plate to record the vertical displacement during the test, as shown in Fig. 4.

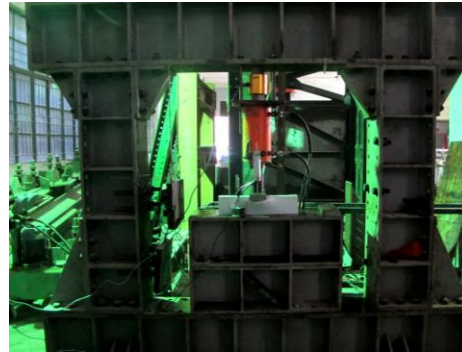


**Figure 2:** Test set-up

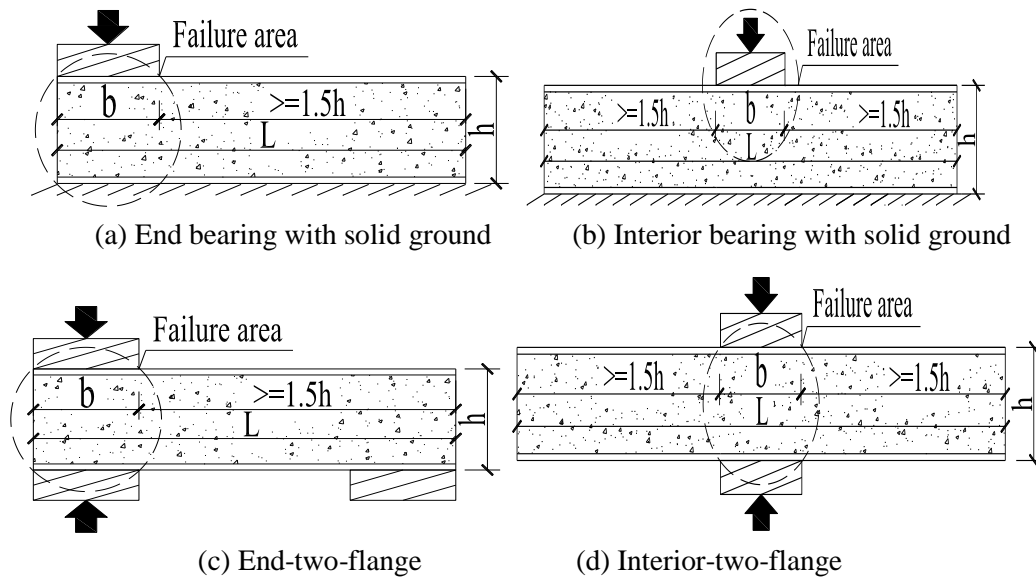


**Figure 3:** Illustration of loading conditions

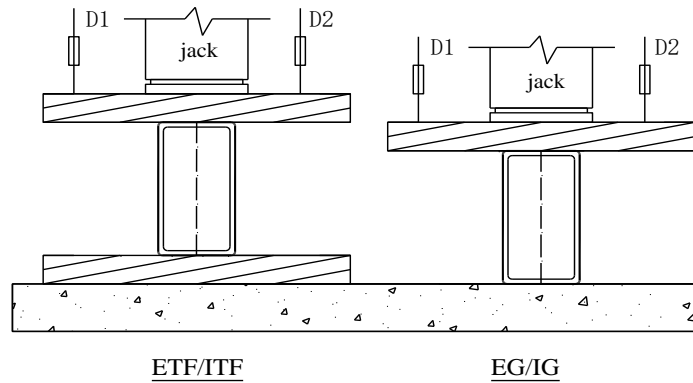


**Figure 4:** Arrangement of displacement transducers

### 3 Test results and analysis

#### 3.1 Failure modes

The failure modes of aluminum hollow specimens were mainly web crippling and the concave deformation of the flange, and the right angle between web and flange was enlarged to obtuse angle. As shown in Figs. 5(a)-5(f), the position and development trend of yield line vary with the different loading conditions.

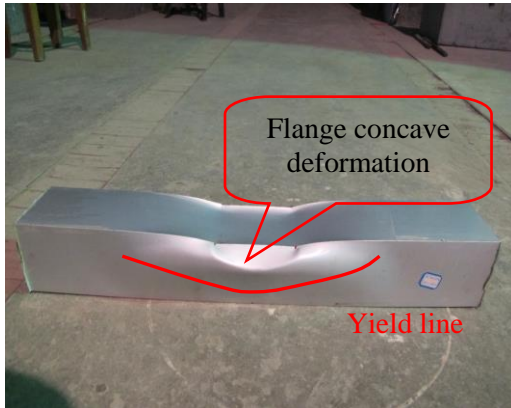
For the composite specimens, web convex deformation and flange extrusion deformation causes the mortar to be crushed and extruded. As the loading conditions change, the position of the yield line and its development trend are also different, as depicted in Figs. 5(g)-5(j).



(a) 110×65-EG-H-150



(b) 110×65-ETF-H-100



(c) 100×100-IG-H-100



(d) 100×100-ITF-H-100



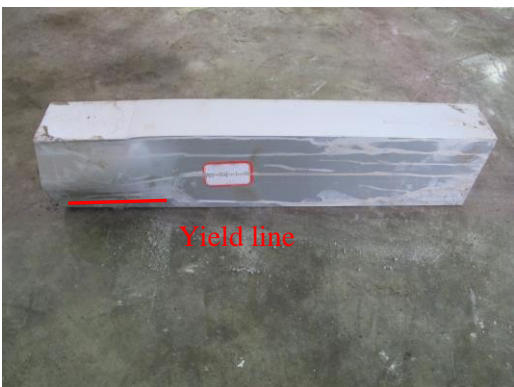
(e) 110×65-IG-H-100



(f) 110×65-ITF-H-100



(g) 110×65-EG-M-100



(h) 110×65-ETF-M-100

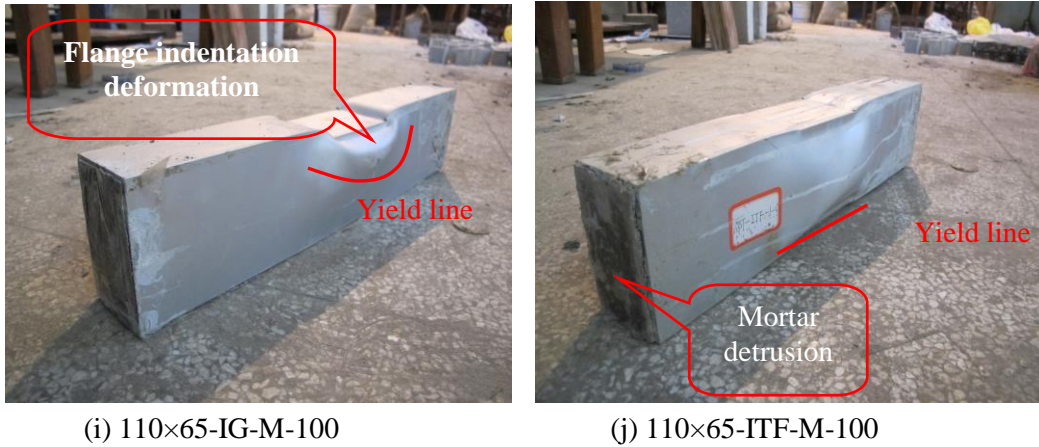
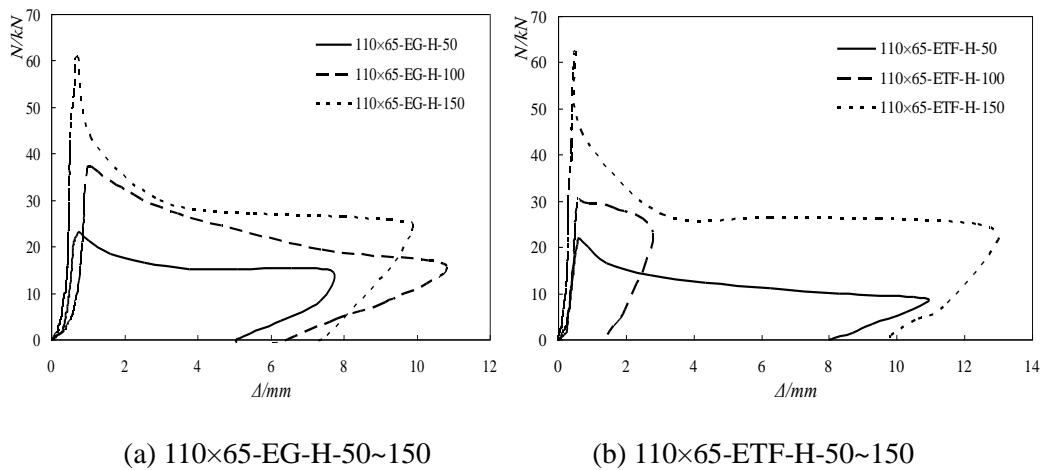
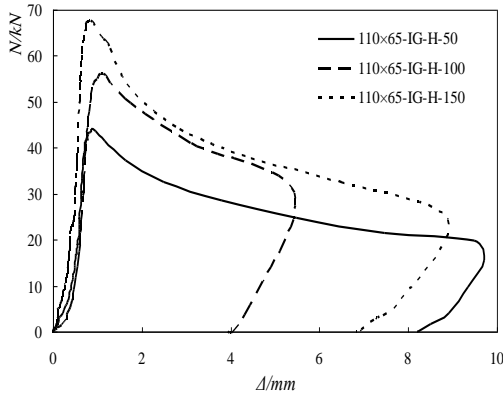


Figure 5: Failure modes of test specimens

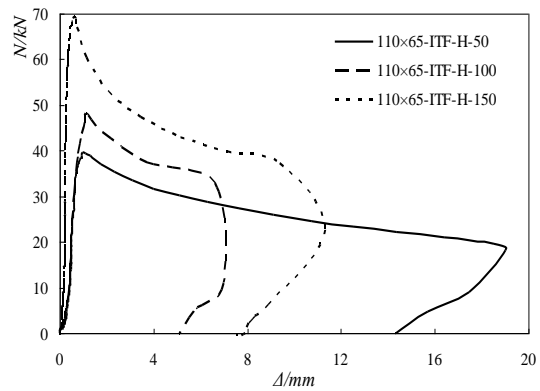
3.2 Load-vertical displacement curves

The load-displacement curves of specimens loaded with different support plate lengths subjected to EG, ETF, IG and ITF loading conditions are shown in Figs. 6(a), 6(b), 6(c) and 6(d), respectively. The complete curve consists of four stages, namely, elastic stage, elastic-plastic stage, plastic stage and unloading stage, where the vertical displacements were obtained by reading of displacement sensors D1 and D2. According to the comparison in Fig. 6, specimens with 150 mm bearing length have maximum ultimate strength and initial stiffness, specimens with 50 mm bearing length and specimens with 100 mm bearing length have almost the same initial stiffness, while the latter have higher ultimate strength.





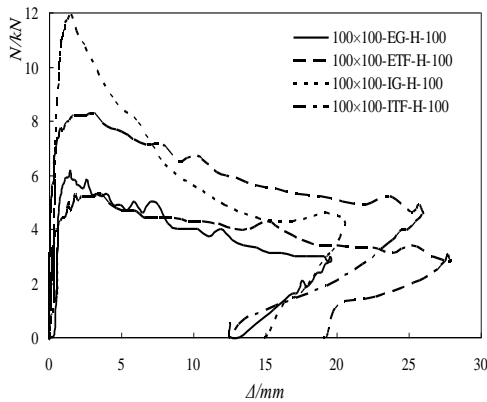
(c) 110×65-IG-H-50~150



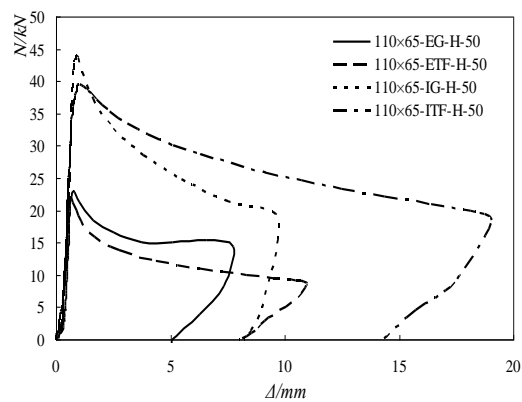
(d) 110×65-ITF-H-50~150

**Figure 6:** Load-displacement curves of specimens with different bearing length

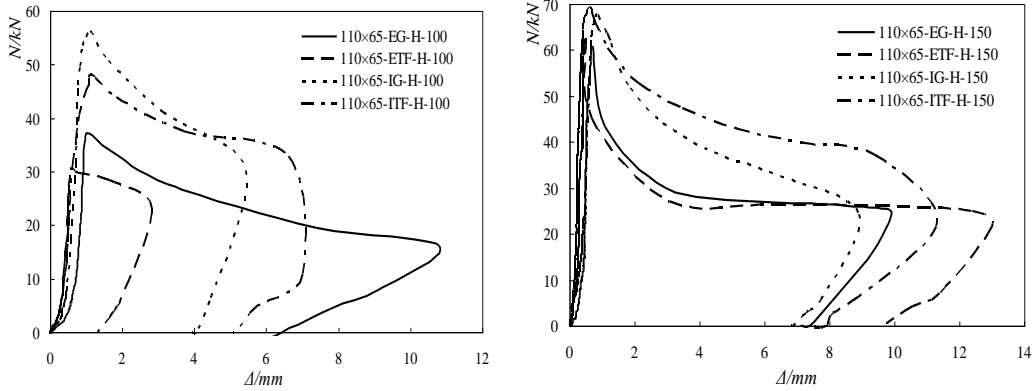
The load-displacement curves of the specimen with different loading conditions are shown in Figs. 7(a)-7(e). It is seen from the comparison in Fig.7 that specimens subjected to interior bearing loading condition have higher ultimate strength and deformation capacity, and the gap narrowed as the bearing length increased. Since the aluminum alloy tube limits the deformation of the mortar, the load of the composite specimen under the internal loading condition increased in the late loading stage.



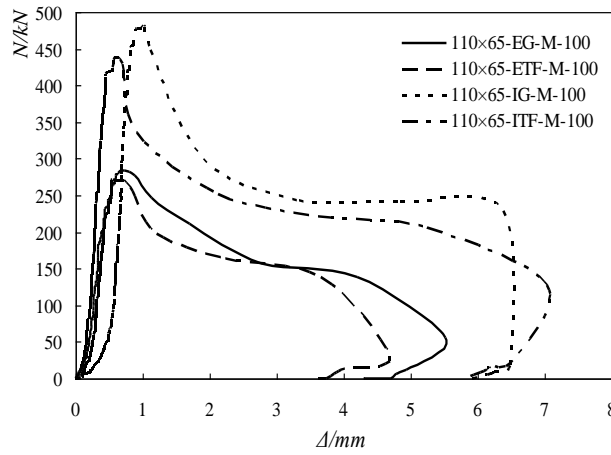
(a) 100×100-Loading Condition-H-100



(b) 110×65-Loading Condition-H-50



(c) 110×65-Loading Condition-H-100      (d) 110×65-Loading Condition-H-150



(e) 110×65-Loading Condition-M-100

**Figure 7:** Load-displacement curves of specimens subjected to different loading conditions

The load-displacement curves of specimens with different slenderness ratio subjected to EG, ETF, IG and ITF loading conditions are shown in Figs. 8(a), 8(b), 8(c) and 8(d), respectively. The specimens with a smaller slenderness ratio have higher ultimate strength and greater initial stiffness, but the ductility is relatively lower.

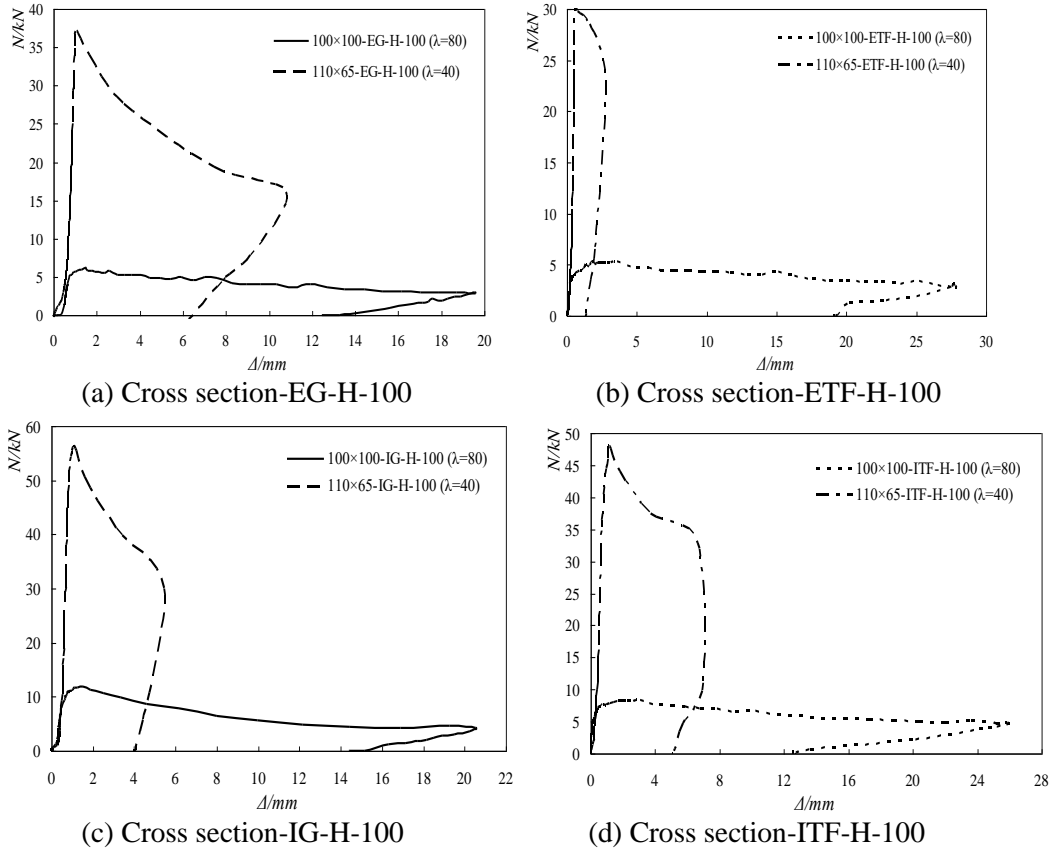


**Figure 8:** Load-displacement curves of steel specimens with different slenderness ratio

### 3.3 Effects of influential factors

The effect of bearing length on the web crippling strength and performance of aluminum hollow section subjected to concentrated load was evaluated, as shown in Tab. 4 and Fig. 9(a). It is inferred from the comparison results that as the length of the bearing plate increases, the ultimate strengths of the specimens improve, and the increase is larger for the specimens under end bearing loading condition.

The enhancement of web crippling strength of aluminum hollow section by infilling the mortar as composite section was evaluated, as shown in Tab. 5 and Fig. 9(b). It is inferred from the comparison results that infilling the aluminum hollow tube with concretes is an effective method for enhancing the ultimate bearing capacity of the web, and the effect is more obvious for the specimens subjected to ITF loading condition.

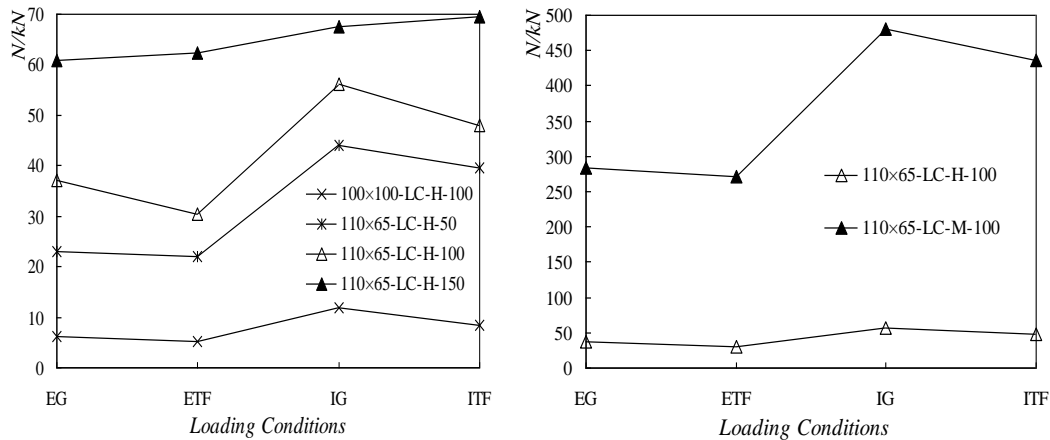
**Table 4:** Comparison results of ultimate strengths of specimens with different bearing lengths

110×65-Loading Conditions-H-b					
Loading Conditions	$P_{us}$ (b=50 mm) (kN)	$P_{us}$ (b=100 mm) (kN)	$P_{us}$ (b=150 mm) (kN)	$P_{us}$ (b=100 mm)/ $P_{us}$ (b=50 mm)	$P_{us}$ (b=150 mm)/ $P_{us}$ (b=50 mm)
EG	23.0	37.2	60.8	1.62	2.64
ETF	21.9	30.5	62.4	1.39	2.85
IG	44.0	56.2	67.6	1.28	1.54
ITF	39.6	48.0	69.4	1.21	1.75
			Mean	1.375	2.195
			COV	0.130	0.295

**Table 5:** Comparison results of ultimate strengths between aluminum hollow specimens and composite specimens

Loading Conditions	EG	ETF	IG	ITF
Aluminum Specimens	110×65-EG-H-100	110×65-ETF-H-100	110×65-IG-H-100	110×65-ITF-H-100
Ultimate strength $P_{us}$ (kN)	37.2	30.5	56.2	48.0
Composite Specimens	110×65-EG-M-100	110×65-ETF-M-100	110×65-IG-M-100	110×65-ITF-M-100
Ultimate strength $P_{uc}$ (kN)	283.6	270.5	479.9	436.7
Comparison $P_{uc}/P_{us}$	7.62	8.87	8.54	9.10

The influence of different load conditions and web slenderness ratios on the web crippling strength and performance of aluminum hollow section under concentrated load was evaluated, as shown Fig. 9(a). It is seen from the comparison that the ultimate strengths of the specimens under interior bearing loads were higher than those of the specimens under end bearing loads. The smaller the slenderness of the specimen, the higher the ultimate bearing capacity of the specimen.



(a) Aluminum hollow specimens      b) Aluminum hollow and composite specimens

**Figure 9:** Ultimate load-loading condition curves

## 4 Finite element analysis

### 4.1 General

The non-linear numerical analysis of aluminum hollow and composite tubes subjected to web crippling was carried out by the finite element program ABAQUS version 6.11. Finite element analysis can be used to model material and geometric nonlinearity. To obtain the exact test results by reasonable computational cost, mesh size of the aluminum tube and the element type, load bearing plates and filled mortar were attentively defined by the convergence research to simulate all specimens. In the finite element analysis, the modeling of materials, the interfaces between aluminum tube and filled mortar, the loading and boundary conditions and the interfaces between aluminum tube and load bearing plates were all taken into account.

The main purpose of finite element analysis was to study the applicability of traditional FE numerical models to simulate the web crippling performance in aluminum hollow and composite tubes, and to replicate the test results. This study was conducted to estimating the ultimate loads and failure modes for each test series. In the framework of ABAQUS standard commercial software [Hibbit, Karlsson and Sorensen (2006)], the finite element models for simulating various types of laboratory web crippling tests are established, and the numerical results were compared with the experimental data.

### 4.2 Mesh and material property

Based on the values measured by the laboratory test, the geometry and sizes of aluminum composite tube and load bearing plates were determined. The models of aluminum composite tube and load bearing plate were established by using C3D8R elements. The C3D8R element is an 8-node solid element with reduced integration. The size of the finite element mesh ranges from 2×2 mm (length by width) to 6×8 mm.

Both elastic and strength properties obtained from the mechanical characteristic experimental results were accustomed to simulate the aluminum composite tube material. In this paper, nonlinear effects are discussed in terms of material and geometric nonlinearities. The steel load-bearing plate was regarded as a linear elastic material having Young's modulus of 210 GPa and Poisson's ratio of 0.31. The representative finite element mesh of aluminum composite tube was shown in Fig. 10.

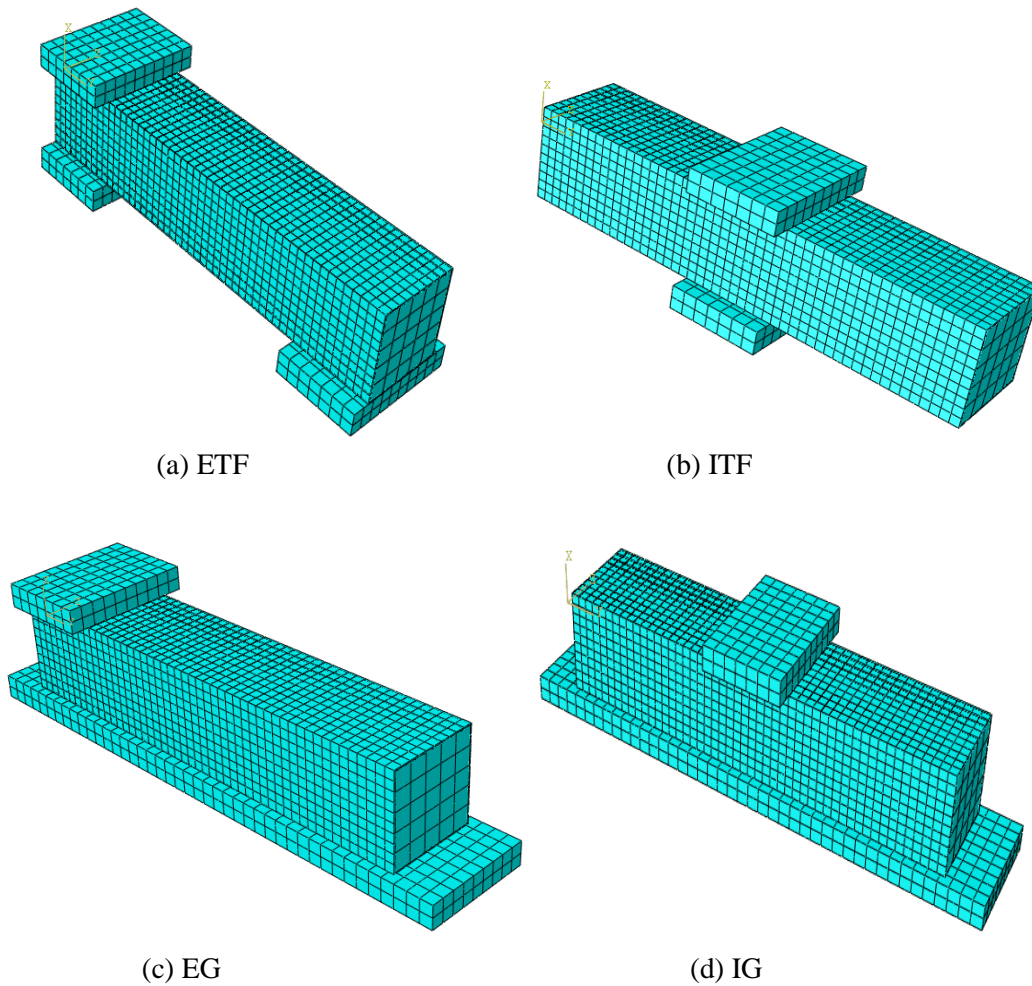


**Figure 10:** Representative finite element mesh of aluminum composite tubes

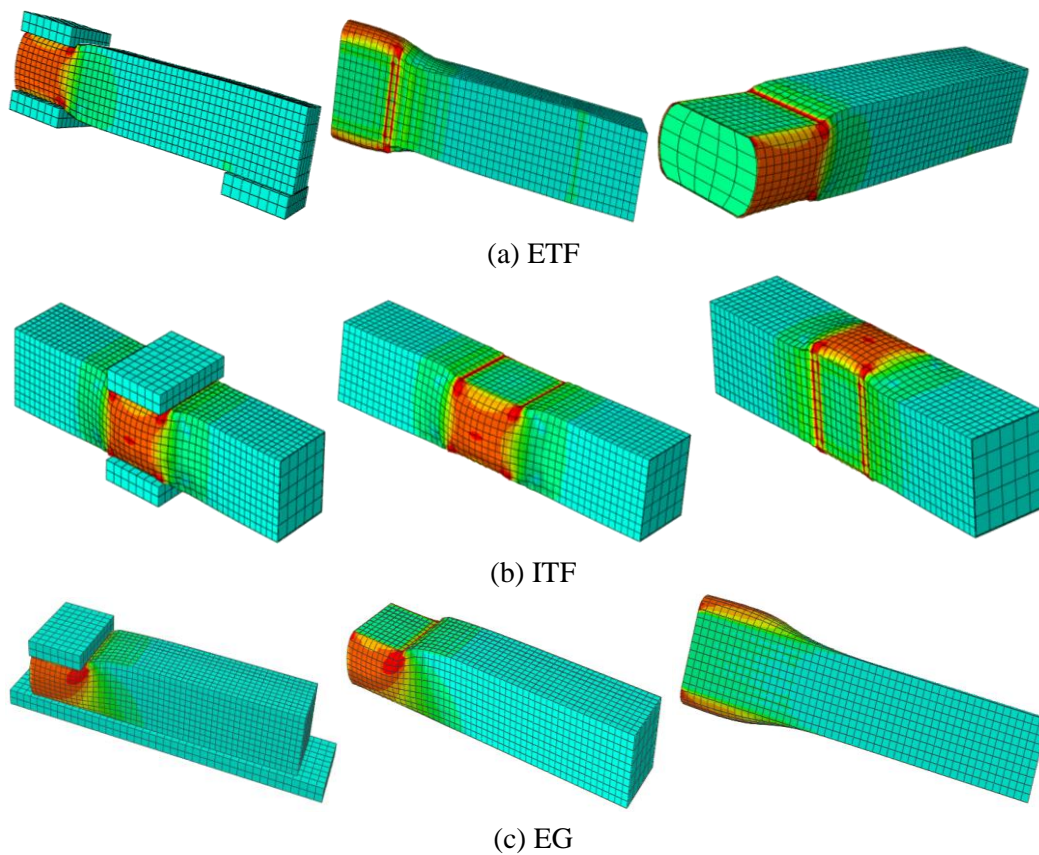
#### **4.3 Loading and boundary conditions**

The boundary conditions and loads were only applicable to the steel bearing plates. In addition to the translation degrees of freedom in the Y direction, the lower surface of the bottom steel plate was subjected to various degrees of freedom. While the higher surface of the upper steel plate was restrained along the horizontal two axes. The interfaces between the bearing plates and the aluminum section were modeled using the contact pair. In linear

buckling analysis, the load acted on the upper steel plate through vertical pressure. In the non-linear analysis, the load was carried out by applying displacement in the vertical direction.

#### **4.4 Verification of FEM**

Finite element models were established subjected to EG, IG, ETF and ITF loading conditions. It is essential to validate the FEM models of grouted aluminum tube subjected to web crippling. In the finite element validation, 16 aluminum hollow tubes and 4 aluminum composite tubes under web crippling were analyzed. The test results were compared with the finite element results, mainly to verify the correctness of the finite element method. The finite element results were verified against the experimental results in the field of failure modes and ultimate capacities. The failure modes obtained by the finite element method in Fig. 11 are compared with those of the experimental tests in Fig. 5. It is found that the failure modes obtained by the finite element method are consistent with the experimental results. The comparison between the ultimate capacity of each specimen obtained from the experimental test and the results of finite element analysis was shown in Table 6. The experimental results are in good agreement with the results of finite element analysis. The maximum error is 8.17%, and the minimum error is 1.88%. Therefore, in terms of web crippling ultimate strength and failure mode, the experimental results are in good agreement with the finite element simulation results.



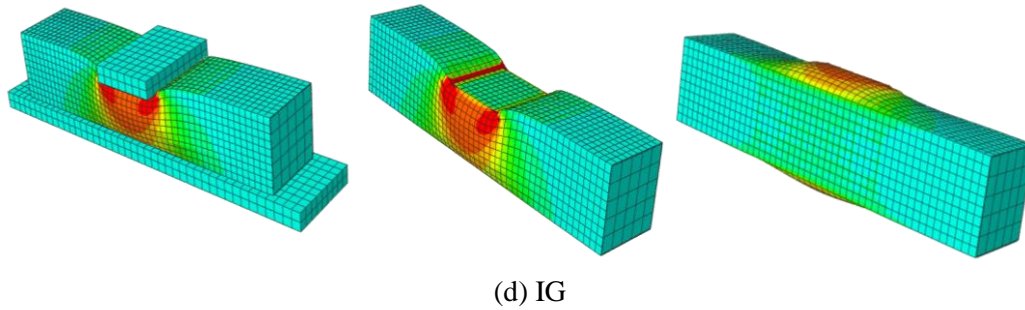


**Figure 11:** Finite element failure modes of aluminum composite tubes under web crippling

**Table 6:** Comparison of Ultimate capacities between finite element models and tests

Specimens	$N_{TEST}$ (kN)	$N_{FEA}$ (kN)	Error (%)
100×100-EG-H-100	6.2	6.6	5.97
100×100-ETF-H-100	5.3	5.4	1.88
100×100-IG-H-100	11.9	12.7	6.72
100×100-ITF-H-100	8.3	8.8	6.02
110×65-EG-H-50	23	23.9	3.91
110×65-EG-H-100	37.2	38.8	4.30
110×65-EG-H-150	60.8	63.6	4.60
110×65-ETF-H-50	21.9	23.5	7.31
110×65-ETF-H-100	30.5	32.9	7.86
110×65-ETF-H-150	62.4	67.5	8.17
110×65-IG-H-50	44	45.8	4.09
110×65-IG-H-100	56.2	59.8	6.40
110×65-IG-H-150	67.6	72.1	6.65
110×65-ITF-H-50	39.6	41.1	3.78

110×65-ITF-H-100	48	50.3	4.79
110×65-ITF-H-150	69.4	72.8	4.89
110×65-EG-M-100	283.6	298.6	5.28
110×65-ETF-M-100	270.5	283.4	4.76
110×65-IG-M-100	479.9	514	7.10
110×65-ITF-M-100	436.7	453.2	3.77

#### 4.5 Parametric research

An extensive parametric research was conducted to study the influence of various parameters such as loading condition, geometric parameters and grout strength on the structural performance of aluminum composite specimens subjected to web crippling by finite element analysis. In this parametric research, 144 aluminum composite tubes models were established. All aluminum composite tube models are set to a height of 200 mm. Considering the practical application, the section size of composite tubes has a large range, as shown in Tab. 7.

**Table 7:** Range of parameters in finite element analysis

Parameters	Values			
Loading conditions	IEF	ETF	IG	EG
$\lambda$	60.0	40.0	100.0	80.0
$b/t_w$	20.0	10.0	40.0	30.0
$H/B$		1.0		2.0
Mortar strength(Mpa)	30.0	20.0		40.0

The bilinear material model includes tensile yield stress ( $f_y$ ) of 190 MPa, Poisson's ratio ( $\nu$ ) of 0.31 and the elastic modulus ( $E$ ) of 70 GPa, which were used for parametric researches of aluminum tubes. Some dimensionless geometric parameters are also involved in the parameter research, including height to width ratio ( $H/B$ ), bearing length to web thickness ratio ( $b/t_w$ ) and slenderness ratio of web ( $\lambda=(H-2t_f-2r)/t_w$ ). The effects of different nominal compressive cube strengths of 20 MPa, 30 MPa and 40 MPa on grouting properties were studied. In the parameter research, four different loading conditions including ETF, ITF, EG and IG are also discussed.

**5 Design rules**

Based on the design formula of cold-formed section steel of single web subjected to local transverse load in Eurocode3 standard, the following four simplified design formulas for predicting web crippling strength of aluminum hollow section under four load conditions are proposed in this paper. Tab. 8 shows the comparison between the predicted web crippling strengths of aluminum tube by the formula and the test values.

$$N_{EGS} = 0.91 \left[ 6 - \frac{(H - 2t_f - 2r)/t_w}{130} \right] \left[ 1 + 0.021 \times \frac{b}{t_w} \right] t_w^2 f_y \tag{1}$$

$$N_{IGS} = 0.92 \left[ 15 - \frac{(H - 2t_f - 2r)/t_w}{50} \right] \left[ 1 + 0.009 \times \frac{b}{t_w} \right] t_w^2 f_y \tag{2}$$

$$N_{ETFS} = 0.86 \left[ 6 - \frac{(H - 2t_f - 2r)/t_w}{60} \right] \left[ 1 + 0.024 \times \frac{b}{t_w} \right] t_w^2 f_y \tag{3}$$

$$N_{ITFS} = 0.91 \left[ 20 - \frac{(H - 2t_f - 2r)/t_w}{16} \right] \left[ 1 + 0.007 \times \frac{b}{t_w} \right] t_w^2 f_y \tag{4}$$

$N_{EGS}$ -Web crippling ultimate strength of aluminum hollow tube subjected to EG loads

$N_{IGS}$ -Web crippling ultimate strength of aluminum hollow tube subjected to ETF loads

$N_{ETFS}$ -Web crippling ultimate strength of aluminum hollow tube subjected to ITF loads

$N_{ITFS}$ -Web crippling ultimate strength of aluminum hollow tube subjected to IG loads

**Table 8:** Ultimate capacities of experimental tests and predicted Strengths by the formulas

Specimen	Loading condition	Bearing length	Ultimate capacity	Predicted ultimate strengths		Comparison
				(Proposed Formulas)		
			$N_u$ (kN)	$N_p$ (kN)	$N_p/N_u$	
100×100-EG-H-100	EG	100	6.2	2.98	0.48	
100×100-ETF-H-100	ETF	100	5.3	2.82	0.53	
100×100-IG-H-100	IG	100	11.9	5.09	0.43	
100×100-ITF-H-100	ITF	100	8.3	4.41	0.53	
110×65-EG-H-50	EG	50	23	8.87	0.39	
110×65-EG-H-100	EG	100	37.2	11.34	0.30	
110×65-EG-H-150	EG	150	60.8	13.80	0.23	
110×65-ETF-H-50	ETF	50	21.9	8.40	0.38	

110×65-ETF-H-100	ETF	100	30.5	11.12	0.36
110×65-ETF-H-150	ETF	150	62.4	13.85	0.22
110×65-IG-H-50	IG	50	44	19.06	0.43
110×65-IG-H-100	IG	100	56.2	22.13	0.39
110×65-IG-H-150	IG	150	67.6	25.20	0.37
110×65-ITF-H-50	ITF	50	39.6	21.59	0.55
110×65-ITF-H-100	ITF	100	48	23.48	0.49
110×65-ITF-H-150	ITF	150	69.4	25.38	0.37
110×65-EG-M-100	EG	100	283.6	131.59	0.46
110×65-ETF-M-100	ETF	100	270.5	131.37	0.49
110×65-IG-M-100	IG	100	479.9	142.38	0.30
110×65-ITF-M-100	ITF	100	436.7	143.73	0.33
				Mean	0.40
				COV	0.238

Based on the research results of numerical parameters, considering the effects of depth-width ratio on mortar strength and the restriction of aluminium tube on mortar deformation, four simplified formulas are proposed to predict web crippling strength of aluminium composite tube under four different loading conditions. The predicted strength is in good agreement with the experimental strength, as shown in Tab. 9.

$$N_{EGC} = \alpha(N_{EGS} + \mu \times f_{mu} \times A) \quad (5)$$

$$N_{IGC} = \alpha(N_{IGS} + \mu \times f_{mu} \times A) \quad (6)$$

$$N_{ETFC} = \alpha(N_{ETFS} + \mu \times f_{mu} \times A) \quad (7)$$

$$N_{ITFC} = \alpha(N_{ITFS} + \mu \times f_{mu} \times A) \quad (8)$$

Among them,  $\alpha$  is the lateral constraint coefficient. When the specimen is subjected to end bearing loads, the value of alpha is 1.7; when the specimen is subjected to internal bearing loads, the value of alpha is 2.7.  $\mu$  is the influence coefficient of depth-width ratio (H/B). When H/B=1.00, the value of  $\mu$  is 1.00, and when H/B=2, the value of  $\mu$  is 0.85.

$N_{EGC}$ -Web crippling ultimate strength of composite specimen subjected to EG loads

$N_{IGC}$ -Web crippling ultimate strength of composite specimen subjected to IG loads

$N_{ETFC}$ -Web crippling ultimate strength of composite specimen subjected to ETF loads

$N_{ITFC}$ -Web crippling ultimate strength of composite specimen subjected to ITF loads

$f_y$ -Tensile yield stress of aluminum hollow sections

$H$ -Profile depth of aluminum hollow sections

*B*-Profile width of aluminum hollow sections

$t_f$ -Flange thickness of aluminum hollow sections

$t_w$ -Web thickness of aluminum hollow sections

*b*-Bearing length

$f_{mu}$ -Cube strength of mortar

Tab. 9 shows the comparison results between the design strength calculated by formulas (5-8) and the design strength obtained by parameter research. The average of the ratio of design formula strength to finite element strength is 0.88, and the corresponding coefficient of variation is 0.085, which indicates that the calculation results of the formula and the research results of the parameters have a good consistency. Therefore, the design formulas presented in this paper are accurate and safe for the design of aluminium composite sections subjected to web crippling.

**Table 9:** Statistics of comparison between design strengths and FEA results

Specimens	Comparison	
A total of 144 aluminum composite tubes	Max	1.23
	Min	0.66
	Mean	0.88
	COV	0.085
EG	Max	1.31
	Min	0.61
	Mean	0.87
	COV	0.083
ETF	Max	1.32
	Min	0.68
	Mean	0.91
	COV	0.084
IG	Max	1.28
	Min	0.65
	Mean	0.85
	COV	0.091
ITF	Max	1.29
	Min	0.64
	Mean	0.86
	COV	0.079

## 6 Conclusions

In this paper, the web crippling tests of aluminum hollow tubes under transverse concentrated loads are carried out, and a method to improve the web crippling strengths

by filling aluminum tubes with concrete is discussed. Based on the above experimental results and parameter studies, the following conclusions can be drawn:

- (1) The failure modes of aluminum hollow specimens were mainly web crippling and the concave deformation of the flange, and the right angle between web and flange was enlarged to obtuse angle. For the composite specimens, web convex deformation and flange extrusion deformation causes the mortar to be crushed and extruded. The position and development trend of yield line vary with the different loading conditions.
- (2) The effect of bearing length on the web crippling strength and performance of aluminum hollow section subjected to concentrated load was evaluated. As the length of the bearing plate increases, the ultimate capacity of the specimens also increases, especially for the specimens under end bearing loading condition.
- (3) Infilling the aluminum hollow tube with concretes is an effective method for enhancing the ultimate bearing capacity of the web, and the effect is more obvious for the specimens subjected to ITF loading condition.
- (4) The influence of different load conditions and web slenderness ratios on the web crippling strength and performance of aluminum hollow section under concentrated load was discussed. The ultimate strengths of the specimens under interior bearing loads were higher than those of the specimens under end bearing loads. The smaller the slenderness of the specimen, the higher the ultimate bearing capacity of the specimen.
- (5) Based on the design formula of cold-formed section steel of single web subjected to local transverse load in Eurocode3 standard, the following four simplified design formulas for predicting web crippling strength of aluminum hollow section under four load conditions are proposed in this paper. Based on the research results of numerical parameters, considering the effects of depth-width ratio on mortar strength and the restriction of aluminium tube on mortar deformation, four simplified formulas are proposed to predict web crippling strength of aluminium composite tube under four different loading conditions. The predicted strength is in good agreement with the experimental strength.

**Acknowledgement:** This research work has been supported by the National Natural Science Foundation of China (Nos. 51478047 and 51778066), the Natural Science Foundation of Hubei Province (No. 2018CFB730) and Foundation project of College of engineering and technology, Yangtze University (No. 2017KY06). Thanks to the support of the laboratory staff.

## References

- Asraf, U.; James, B. P. L; David, N.; Jim, R; Young, B. (2012): Cold-formed steel sections with web openings subjected to web crippling in two-flange loading conditions-Part II: Parametric study and proposed design equations. *Thin-Walled Structures*, vol. 56, no. 7, pp. 79-87.
- Asraf, U.; James, B. P. L; David, N.; Jim, R.; Young, B. (2012): Web crippling behaviour of cold-formed steel channel sections with offset web holes subjected to interior-two-flange loading. *Thin-Walled Structures*, vol. 50, no. 1, pp. 76-86.

**American Society of Civil Engineers** (2002): *Specification for the Design of Cold-Formed Stainless Steel Structural Members, SEI/ASCE-8-02*. American Society of Civil Engineers.

**Australia Standards Association of Australia** (2001): *Cold-Formed Stainless Steel Structures AS/NZS 4673-2001*, Standards Australia International Ltd.

**Bock, M.; Real, E.** (2014): Strength curves for web crippling design of cold-formed stainless steel hat sections. *Thin-Walled Structures*, vol. 85, no. 12, pp. 93-105.

**Chen, Y.; Chen, X. X.; Wang, C. Y.** (2015): Experimental and finite element analysis research on cold-formed steel lipped channel beams under web crippling. *Thin-Walled Structures*, vol. 87, no. 2, pp. 41-52.

**Chen, Y.; Wang, C. Y.** (2015): Test on pultruded GFRP I-section under web crippling. *Thin-Walled Structures*, vol. 77, no. 8, pp. 27-37.

**Chen, Y.; Wang, C. Y.** (2015): Web crippling behavior of pultruded GFRP rectangular hollow sections. *Composites Part B*, vol. 77, no. 8, pp. 112-121.

**Chen, Y.; Chen, X. X.; Wang, C. Y.** (2016): Web crippling of galvanized steel tube strengthened by CFRP sheets. *Composites Part B*, vol. 84, no. 1, pp. 200-210.

**He, K.; Chen, Y.; Wan, J.** (2018): Web crippling behavior of grouted galvanized rectangular steel tube. *Thin-Walled Structures*, vol. 122, no. 1, pp. 300-313.

**Li, H. T.; Young, B.** (2017): Tests of cold-formed high strength steel tubular sections undergoing web crippling. *Thin-Walled Structures*, vol. 141, no. 6, pp. 571-583.

**Hibbitt; Karlsson; Sorensen** (2006): *ABAQUS. Standard User's Manual*. Version 6.11. Vols. 1-3, USA.

**Islam, S. M. Z; Young, B.** (2018): Design of CFRP-strengthened aluminium alloy tubular sections subjected to web crippling. *Thin-Walled Structures*, vol. 124, no. 3, pp. 605-621.

**Islam, S. M. Z; Young, B.** (2012): Web crippling of aluminium tubular structural members strengthened by CFRP. *Thin-Walled Structures*, vol. 59, no. 10, pp. 58-69.

**Islam, S. M. Z.; Young, B.** (2013): Strengthening of ferritic stainless steel tubular structural members using FRP subjected to Two-Flange-Loading. *Thin-Walled Structures*, vol. 62, no. 1, pp. 179-190.

**Islam, S. M. Z; Young, B.** (2014): FRP strengthening of lean duplex stainless steel hollow sections subjected to web crippling. *Thin-Walled Structures*, vol. 85, no. 12, pp. 183-200.

**Islam, S. M. Z; Young, B.** (2011): FRP strengthened aluminium tubular sections subjected to web crippling. *Thin-Walled Structures*, vol. 49, no. 11, pp. 1392-1403.

**Lavan, S.; Mahen, M.; Poologanathan, K.** (2017): Web crippling experiments of high strength lipped channel beams under one-flange loading. *Journal of Constructional Steel Research*, vol. 138, no. 11, pp. 851-866.

**Lourenço, A. F.; José, G.; João, R. C.; Nuno, S.; Francisco, N.** (2015): Web-crippling of GFRP pultruded profiles. Part 1: Experimental study. *Composite Structures*, vol. 120, no. 2, pp. 565-577.

**National Standard of the People's Republic of China** (2002): *Metallic Materials-Tensile Testing at Ambient Temperature. GB/T 228-2002*, General Administration of Quality Supervision, Inspection and Quarantine of the People's Republic of China.

**National Standard of the People's Republic of China** (2009): *Standard for Test Method of Performance on Building Mortar. JGJ/T70-2009*, Ministry of Construction of the People's Republic of China.

**Macdonald, M.; Heiyantuduwa, M. A.** (2012): A design rule for web crippling of cold-formed steel lipped channel beams based on nonlinear FEA. *Thin-Walled Structures*, vol. 53, no. 4, pp. 123-130.

**Natário, P.; Silvestre, N.; Camotim, D.** (2016): Direct strength prediction of web crippling failure of beams under ETF loading. *Thin-Walled Structures*, vol. 98, no. 11, pp. 360-374.

**Natário, P.; Silvestre, N.; Camotim, D.** (2014): Web crippling failure using quasi-static FE models. *Thin-Walled Structures*, vol. 84, no. 11, pp. 34-49.

**Wu, C.; Bai, Y.** (2014): Web crippling behaviour of pultruded glass fibre reinforced polymer sections. *Composite Structures*, vol. 108, no. 2, pp. 789-800.

**Wu, C.; Zhao, X. L.; Duan, W. H.** (2011): Design rules for web crippling of CFRP strengthened aluminium rectangular hollow sections. *Thin-Walled Structures*, vol. 49, no. 10, pp. 1195-1270

**Zhao, X. L.; Al-Mahaidi, R.** (2009): Web buckling of light steel beams strengthened with CFRP subjected to end-bearing forces. *Thin-Walled Structures*, vol. 47, no. 10, pp. 1029-1036.

**Zhou, F.; Young, B.** (2006): Cold-formed stainless steel sections subjected to web crippling. *Journal of Structural Engineering ASCE*, vol. 132, no. 1, pp. 134-144.

**Zhou, F.; Young, B.** (2008): Aluminum tubular sections subjected to web crippling-Part I: Tests and finite element analysis. *Thin-Walled Structures*, vol. 46, no. 4, pp. 339-351.

**Zhou, F.; Young, B.** (2010): Web crippling of aluminium tubes with perforated webs. *Engineering Structures*, vol. 32, no. 5, pp. 1397-1410.